Earthquakes in a fault system embedded in an elastic body subject to increasing shear stress (*)

M. Caputo [1], G. Della Monica [2], F. Fattori Speranza [2]
S. Reseda [2] and V. Sgrigna [2]

[1] *Dipartimento di Fisica, Università degli Studi "La Sapienza"*
   P.le A. Moro 2, Roma, I-00185 Italy
[2] *Dipartimento di Fisica "E. Amaldi", Università degli Studi "Roma Tre"*
   Via della Vasca Navale 84, I-00146 Roma, Italy

Summary. — We consider the faults of an elastic body subject to an increasing stress and the stress field generated by slip on a fault. The slip along the fault releases the stress component parallel to the slip, but the component normal to the fault is not released and increases in time at the same rate as the shear affecting the body. The effect is an increase of the value of the force necessary to cause the subsequent slip; and, if the shear increases linearly, it causes an increase of the time intervals between the earthquakes on the fault, that is between the stress drop p and the slip s. The density distribution of p in a given time interval is computed; it is found that rigorously it is not a power law although it is a decreasing function of p. It is also seen that, as in the cases in which it was assumed that the component of the stress field locking the fault, after each earthquake, in the time interval to the next earthquake, would be anelastically released, the logarithm of the density distribution of the moments of the earthquakes is a linear function of $\log(M_0)$ and a linear function of M in any time interval; M_0 and M being the scalar seismic moment and the magnitude, respectively. Conditions for the existence of these linear relationships are discussed finding that a sufficient condition, when the range of p is not exceptionally large, is that the density distribution of p be of the type $\log(p)$, which includes the case when it is independent of the fault linear size l. The Gutenberg-Richter frequency-magnitude relationship and the conditions to obtain aftershocks and seismic swarms generated by this model are presented and discussed. In order to obtain the observed density distribution of earthquakes one or several hypotheses can be done: 1) the stress locking the faults, between successive earthquakes of the same fault, is released anelastically; 2) the density distribution of the sizes of the faults is such as to cause the logarithm of the density distribution of $\log(M_0)$ and of M to be linear; 3) the density distribution of $\log M_0(M)$ is linear and the linearity factor is related to the density distribution of the stress drop and not to that of the linear dimensions of the faults.

PACS 91.30 – Seismology.
PACS 91.35 – Earth's interior structure and properties.

1. – Introduction

The problem of developing physical (or mechanical) and stochastic models for the analysis of earthquake catalogues has raised strong interest during the last decades [1-9].

In many seismic regions the historical record of seismicity is too short to evaluate repeat time or possible clustering of large earthquakes in both space and time. Paleoseismic studies can help to extend the historical record for specific areas, but with large uncertainties and time delays [10]. Moreover, it is difficult to obtain possible precursory seismicity patterns from existing catalogues of earthquakes because of their short duration and inhomogeneity. These facts justified the development of synthetic seismicity models, in which long catalogues of earthquakes are generated by computer models of seismogenesis. One of the most general mathematical models for synthetic seismicity, based upon the hypothesis that earthquakes are fluctuations of plate motions, was developed by Rundle [11]. Some other representative examples of such models are: cellular automata models of two-dimensional faults, which neglect elasticity and fault friction and which reproduce seismic frequency-magnitude statistics (*e.g.*, [12]); spring-block models of one-dimensional or two-dimensional faults, with realistic frictional properties and simplified stress transfer to nearest interactions (*e.g.*, [13]); models of single two-dimensional faults in which slip is divided into patches with simplified frictional laws (*e.g.*, [14]); continuum models of single two-dimensional faults with realistic constitutive frictional laws and details concerning slip nucleation and propagation (*e.g.*, [5]); physical, as opposed to computer, models of the spring-block type (*e.g.*, [3]).

Unfortunately, most of the stochastic models depend on too large a number of parameters to allow the fitting of almost any data in the short range where the data are available. This conclusion is further unsatisfactory because the poor accuracy of the data does not demonstrate which model best fits the observational data.

Knowing this would allow the prediction by extrapolation of other statistical features such as the statistical properties of large earthquakes of the region, which are so rare as to discourage in general any attempt aiming at a reliable result.

On the other hand, most of the mechanical models seem to be too simplistic and often ignore the physical aspects of the earthquake occurrence which are difficult to fit in the model, mostly because of the scarce knowledge of the parameters which physically represent the phenomenon itself. Examples of poorly known parameters are those concerning the asperities, the friction, the amount of stored elastic energy transformed into heat, and the transfer of energy between the gravitational and elastic fields.

Since the theory of the elastic rebound proposed by Reid [15], the earthquake process has not been considered an isolated and unique event episode, but at least all shallow earthquakes with magnitude greater than 6.0 are considered to occur on pre-existing faults. This implies that generally earthquakes represent a repeated rupture (with consequent slip) of an established fault. As a consequence of relative motions on either sides of a fault which cause the locking and unlocking of some of its parts due to friction, strain accumulates and relaxes alternatively along the fault.

The idea that fault failures occur with some periodic behaviour is important for earthquake prediction.

If the tectonic processes which cause the relative motions along faults were steady, the strain accumulation should also be steady. Then, if the shear accumulation on the

fault is assumed to be time independent, earthquakes should occur along faults at almost regular intervals.

Three models for the building-up and releasing of stress on a fault segment have been proposed. They are the above-mentioned regular stick slip faulting (or characteristic earthquake model), the time predictable model, and the slip predictable model.

In the characteristic earthquake model [16, 17] the fault offset would be the same for each event and the recurrence interval is constant. Therefore, in this model the faults are segmented and individual segments behave in a predictable way. Then, the method consists in the classification of seismic gaps by the time elapsed since the last large earthquake. But this behaviour is rarely observed in nature, mainly because the fault mechanical behaviour is not constant and the strain accumulation on a fault is not purely elastic, then tectonic processes may not be steady in a short term.

Due to the non-linear nature of frictional sliding and occurrence of adjacent earthquakes and non-uniform slip, it is fundamental for the maximum stress value on the fault (strength of the fault) and for the minimum stress value after relaxation to be constant.

The condition of constant maximum stress gives rise to the time predictable model for the earthquake behaviour. In this model [18] the stress drop may vary from earthquake to earthquake and, consequently, the time to the next event will vary. The amount of displacement in an event will specify the time interval to the next earthquake. The method consists in the calculation of the expected time of occurrence from slip in the previous earthquake, and long-term slip rates.

In the slip predictable model [19, 20] earthquakes occur over different values of maximum stress, but the fault relaxes to a constant minimum stress value. In this model the lapse time since the last event specifies the potential fault displacement at a given time. That is, the method gives the estimated conditional probability for recurrence of earthquake slip.

In both the last two models an estimate of the long-term relative motion is required.

Even if neither model is perfect, more faults seem to show a weak tendency to exhibit time predictable behaviour. One of the biggest difficulties in determining the characteristics of fault behaviour is that we rarely have more than one or two cycles in the historical records.

It seems that these models are too simplistic and, in general, the mean recurrence time may be well defined, but significant statistical fluctuations occur.

Current methods for calculation of long-term probabilities for the recurrence of large earthquakes on specific fault segments are based upon models of the faulting process that implicitly assume constant stress rates during the interval separating earthquakes and instantaneous failure at a critical stress threshold [21]. A model of the earthquake cycle with variable stressing has also been proposed [21, 22].

It has long been noted that a power law originally proposed by Ishimoto and Iida [23], for seismic amplitudes, and by Gutenberg and Richter [24], for magnitudes, seems to describe the distribution of earthquakes over a large range of seismic magnitudes in seismic regions such as Japan and California.

Triep and Sykes [25] investigated the b-value changes to justify the departure of shallow intracontinental earthquakes from the Gutenberg-Richter frequency-magnitude relationship.

Guo and Ogata [26], on the basis of 34 aftershock sequences occurred in Japan from 1971 to 1995, analysed the correlation between statistical parameters of seismicity,

such as the b-value of the Gutenberg-Richter relation, the p-value of the modified Omori formula [27], the p and α values of the Epidemic Type Aftershock Sequence (ETAS) model [28], and the fractal dimension of the hypocenter distribution.

Since 1976, Caputo [1, 29] has been introducing a mechanical model based on a power law distribution of the linear size of the faults, to explain the Ishimoto-Iida and Gutenberg-Richter empirical laws and a physical meaning to the b-value through the fitting of all the regions of the world for which reliable catalogues of earthquakes exist. Also the statistic of the seismic moment and an estimate of the number and size of faults was explained by this model as well as the maximum magnitude and seismic moment possible in the region. After reviewing the model [30, 31], decreasing power laws were proposed to represent the statistical distributions of the stress drop.

Similar results were also obtained by Davy [32] for the statistical distribution of the linear dimension of faults and by Christensen and Olami [33] for the elastic energy (proportional to the seismic moment) released during the earthquake.

Aki [34] investigated the interrelation between fault zone structures and earthquakes in order to develop capabilities for predicting the earthquake process.

Gabrielov *et al.* [35] suggested a model of interaction of lithospheric blocks producing an artificial catalogue of earthquakes.

In this note a model concerning the density distribution of earthquakes as a function of the scalar seismic moment and strain energy is proposed making use of a linear stress field acting on a fault system with an assigned density distribution of their characteristic linear size.

2. – The case of a linear stress field

First, we will consider a seismic region and the case of an elastic body with a system of faults without any specification on the fault orientation. The case with a parametric fault orientation will be examined in the following section. In the absence of direct information on the distribution of the fault size it seems reasonable to assume, according to Caputo [30], that the number of faults with linear size l ($l = \sqrt{S}$, S is the area of the faults) in the range $(l, l + dl)$ is a decreasing function of l:

$$(1) \qquad\qquad D l^{-\nu}\, dl\,,$$

where D is a positive normalizing factor which represents a constant typical of the seismic region and ν is defined by $\nu = (3b/\gamma) + 1 > 0$, with b and γ ($0.5 < \gamma < 2.0$) obtained from experimental checks [29], as the coefficients of the Gutenberg-Richter law and of the empirical relationship between scalar seismic moment M_0 (or the elastic energy W released by the earthquake) and magnitude M, respectively [31, 36]. The fault is subject to a stress field increasing linearly with time t as $\dot{\sigma} t$ (with dimension $g\, cm^{-1}\, s^{-2}$).

After time t the stress field will cause a force

$$(2) \qquad\qquad f_1 = S(F + f_c \dot{\sigma} t)$$

acting in the direction to lock the fault, and a force

$$(3) \qquad\qquad f_2 = S f_c' \dot{\sigma} t$$

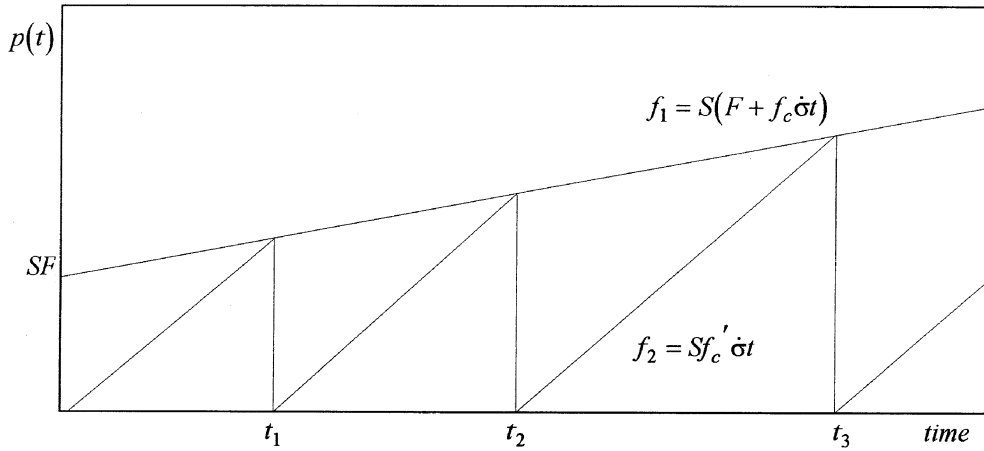acting in the direction to unlock it. Both forces f_1 and f_2 *vs.* time are reported in fig. 1,

Fig. 1. – Stress field increasing linearly in time t as $\dot{\sigma}t$ ($\dot{\sigma}$ being the stress rate) and acting on a fault. The forces f_1, locking the fault, and f_2, acting to unlock it, are also reported in the figure as a function of time t, of cohesive force F per unit area, and of coefficients f_c and f_c' ($f_c < f_c'$). At times $t_1, t_2, t_3, \ldots, f_1 = f_2$, and slips along the fault release all the stresses parallel to the fault; these relaxations will be associated to the stress drops $p(t_1)$, $p(t_2)$, $p(t_3)$, $\ldots$, respectively.

with $f_c \neq f_c'$, and $f_c < f_c'$ (*e.g.*, eq. (26)). They are dimensionless; f_c contains (*e.g.*, eqs. (32)) the frictional coefficient between the faces of the fault and is a function of the fault orientation; f_c' is a function of the fault direction (see eqs. (32)); F is the cohesive force per unit area (with dimensions $g\,cm^{-1}s^{-2}$), acting between the same faces of the fault, and is caused by welding due to heat and pressure; and $\dot{\sigma}$ represents the constant rate of increase of the stress field.

The assumption concerning the locking and unlocking forces f_1 and f_2, as we shall see, will allow us to consider the case in which the elastic body is subject to a shear and the case in which it is subject to a compression. In this paper only the first case will be considered.

Under conditions which will be specified when considering the two particular cases indicated in eqs. (2) and (3), at the time t_1 resulting from the equation

$$(4) \qquad\qquad F + f_c\dot{\sigma}t_1 = f_c'\dot{\sigma}t_1,$$

which gives

$$(5) \qquad\qquad t_1 = \frac{F}{(f_c' - f_c)\,\dot{\sigma}},$$

the locking force and that acting to unlock it will be equal (fig. 1) and, if the slip along the fault releases all the force parallel to it, it will be associated to a stress drop $p(t_1)$ given by

$$(6) \qquad\qquad p(t_1) = f_c'\dot{\sigma}t_1 = F\frac{f_c'}{f_c' - f_c}.$$

The force per unit area locking the fault is

(7)
$$p(t_1) = F + f_c \dot{\sigma} t_1 = F + F \frac{f_c}{f'_c - f_c}$$

and will remain unreleased.

Note that

(8)
$$\dot{\sigma} t_1 = \frac{F}{(f'_c - f_c)} .$$

As both forces increase (eqs. (6) and (7)), at time t_2, solution of the following equation:

(9)
$$F + f_c \dot{\sigma} t_2 = f'_c \dot{\sigma} (t_2 - t_1),$$

the two forces will be again equal and, if a new slip along the fault releases all the stress parallel to the fault, this will be associated to a stress drop $p(t_2)$ given by

(10)
$$p(t_2) = f'_c \dot{\sigma} (t_2 - t_1).$$

The time t_2 is computed from eq. (9) introducing t_1 from eq. (5):

(11)
$$t_2 = F \frac{(2f'_c - f_c)}{(f'_c - f_c)^2 \dot{\sigma}} .$$

Then, the force per unit area acting to unlock the fault related at this time t_2 is

(12)
$$p(t_2) = f'_c \dot{\sigma} (t_2 - t_1) = F \left(\frac{f'_c}{f'_c - f_c} \right)^2 .$$

Note that

(13)
$$\dot{\sigma} (t_2 - t_1) = F \frac{f'_c}{(f'_c - f_c)^2} .$$

Using the same procedure, one may compute the time t_3 when another slip will occur associated to the stress drop $p(t_3)$.

In fact, at time t_3 we have

(14)
$$F + f_c \dot{\sigma} t_3 = f'_c \dot{\sigma} (t_3 - t_2)$$

and introducing in eq. (14) t_2 from eq. (11) we obtain

(15)
$$t_3 = F \frac{3(f'_c)^2 + f_c^2 - 3f_c f'_c}{(f'_c - f_c)^3 \dot{\sigma}} .$$

The force per unit area acting to unlock the fault will be at time t_3

(16)
$$p(t_3) = f'_c \dot{\sigma} (t_3 - t_2) = F \left(\frac{f'_c}{f'_c - f_c} \right)^3 .$$

Note that

$$(17) \qquad \dot{\sigma}(t_3 - t_2) = F \frac{(f_c')^2}{(f_c' - f_c)^3} \, .$$

In general, assuming that

$$(18) \qquad \beta = \frac{f_c'}{f_c' - f_c} \, ,$$

we obtain

$$(19) \qquad \begin{cases} \dot{\sigma}(t_n - t_{n-1}) = F \dfrac{(f_c')^{n-1}}{(f_c' - f_c)^n} = \dot{\sigma}t_1 \left(\dfrac{f_c'}{f_c' - f_c} \right)^{n-1} = \dot{\sigma}t_1 \beta^{n-1}, \\[2ex] p(t_n) = F \left(\dfrac{f_c'}{f_c' - f_c} \right)^n = F\beta^n \end{cases}$$

and repeating the same procedure it can be seen that formulae (19) are valid also for $n + 1$ and this proves that they are valid for any n.

We have assumed here that at any t_n the stress along the fault drops to zero (see also fig. 1).

We note that the time t_n is the sum of all t_k from $k = 0$ through $k = n$, therefore

$$(20) \qquad \dot{\sigma}t_n = \dot{\sigma}[t_1 + (t_2 - t_1) + (t_3 - t_2) + \dots + (t_n - t_{n-1})] = \dot{\sigma}t_1(1 + \beta + \dots + \beta^{n-1}) =$$

$$= \dot{\sigma}t_1 \sum_{k=0}^{n-1} \beta^k = \dot{\sigma}t_1 \frac{(1 - \beta^n)}{(1 - \beta)} \, ,$$

and introducing in eq. (20) $\dot{\sigma}t_1$ from eq. (8) we obtain

$$(21) \qquad \dot{\sigma}t_n = F \frac{(1 - \beta^n)}{(f_c' - f_c)(1 - \beta)} = F \frac{\beta(1 - \beta^n)}{f_c'(1 - \beta)} = F \frac{(1 - \beta^n)}{f_c'(1/\beta - 1)} = F \frac{(\beta^n - 1)}{f_c} \, .$$

Finally, summarising the results from eqs. (19) and (21) we can write

$$(22) \qquad \begin{cases} \dot{\sigma}t_n = F \dfrac{\beta^n - 1}{f_c} \, , \\[2ex] \dot{\sigma}(t_n - t_{n-1}) = \dot{\sigma}t_1 \beta^{n-1} = F \dfrac{\beta^n}{f_c'} \, , \\[2ex] p(t_n) = F + f_c \dot{\sigma}t_n = F\beta^n \, . \end{cases}$$

The number n of earthquakes in the catalogue is obtained considering the maximum value of t_n contained in T_1 and then solving the following inequality in n:

$$(23) \qquad \dot{\sigma}T_1 > \dot{\sigma}t_n = F \frac{\beta^n - 1}{f_c} \, ,$$

which gives the largest integer n:

$$(24) \qquad n < \frac{\log\left[(1 + \dot{\sigma}T_1 f_c)/F\right]}{\log\beta} \, .$$

Since from eq. (24) β must be positive, it is found from eq. (18) that

$$(25) \qquad f_c < f_c' \, .$$

Then, $1/\beta = 1 - (f_c/f_c') < 1$, and $\beta > 1$. Inequality (25) implies different values for the coefficients of the linear relationships (2) and (3) and, consequently, different slopes for the two straight lines of fig. 1 representing the same forces f_1 and f_2.

In practice, one tries the values of n in eq. (22) choosing the largest value of n fitting the condition (23) set with T_1.

In fact, it is important to note that the time t_n is not necessary for the compilation of the statistical catalogue, but only the number n is.

Naturally, the cumulative distribution of n is not a linear function of T_1. Taking it from eq. (24), since $\dot{\sigma}T_1 f_c/F \gg 1$, differentiating with respect to T_1 one obtains that the temporal density distribution of the number of earthquakes per unit time is proportional to $1/T_1$, which is Omori's type law:

$$(26) \qquad \frac{\mathrm{d}n}{\mathrm{d}T_1} = \frac{1}{\log\beta} \frac{f_c\dot{\sigma}}{(F + f_c\dot{\sigma}T_1)} = \frac{1}{\log\beta} \frac{1}{(F/f_c\dot{\sigma} + T_1)} \propto \frac{1}{T_1} \, .$$

This relationship is valid with the already stated assumption of absence of relaxation and resembles the condition of occurrence of aftershocks.

The density distribution of stress drops as a function of stress drop (p) is given by eqs. (19) and (22): but eqs. (19) and (22), without knowledge of t, which implies the knowledge of $\dot{\sigma}$, will give no indications on the average return period of the stress drops.

However, these formulae allow us to see that the density distribution of the stress drops on the same fault is inversely proportional to the stress drop. In fact, from eq. (22) we consider $p(t_n) = Fe^{n\ln\beta}$ which relates n to the stress drop at time t_n, or the cumulative number of stress drops at time t_n. Differentiating with respect to n, we obtain

$$(27) \qquad \frac{\mathrm{d}p}{\mathrm{d}n} = F\ln\beta e^{n\ln\beta} = F\beta^n \ln\beta = p(t_n)\ln\beta \, ,$$

which gives the density distribution of the number of stress drops:

$$(28) \qquad \frac{\mathrm{d}n}{\mathrm{d}p} = \frac{1}{p(t_n)\ln\beta} \, ,$$

that is inversely proportional to the stress drop $p(t_n)$. We will see in the following that when introducing the scalar seismic moment M_0, eq. (28) constitutes the Gutenberg-Richter relationship.

The data analysis of Caputo [30, 31] on 16 sets of data in different regions of the world indicates that instead of $1/p$ the density distribution (28) is of the type $1/p^{(1-\alpha)}$

with $-1 < \alpha < 0$, which favours the smaller stress drops and confirms eq. (28) in few cases, mainly in aftershocks.

3. – The case of shear stress

We will now specify the generic model considered in the previous paragraph to the case when the body is still subject to a shear stress varying in time as $\dot{\sigma}t$, but choosing the coordinate axes (x_1, x_2, x_3) such that the shear is parallel to x_1 and in the (x_1, x_2)-plane, and the faults are parallel to x_3 (fig. 2). In this co-ordinate system the faults are identified by the angle θ of their normal $\widehat{n} = -\sin\theta, \cos\theta, 0)$ with the x_2-axis measured anticlockwise. The faults slip is identified by $\widehat{l} = (\cos\theta, \sin\theta, 0)$.

This case is a generalisation of that considered by Caputo and Caputo [36] in which it was assumed that after each event, the locking force would become nil.

In the present case the applied stress is

$$
(29) \quad \tau\widehat{l} = \begin{pmatrix} \varrho gh & \dot{\sigma}t & 0 \\ \dot{\sigma}t & \varrho gh & 0 \\ 0 & 0 & \varrho gh \end{pmatrix} \begin{pmatrix} \cos\theta \\ \sin\theta \\ 0 \end{pmatrix} = \begin{pmatrix} \varrho gh \cdot \cos\theta + \dot{\sigma}t \cdot \sin\theta \\ \dot{\sigma}t \cdot \cos\theta + \varrho gh \cdot \sin\theta \\ 0 \end{pmatrix} = \vec{\tau},
$$

$$
(30) \quad \vec{\tau} \cdot \widehat{n} = (-\varrho gh \cdot \cos\theta \cdot \sin\theta - \dot{\sigma}t \cdot \sin^2\theta + \dot{\sigma}t \cos^2\theta + \varrho gh \cdot \sin\theta \cdot \cos\theta) =
$$

$$
= \dot{\sigma}t(\cos^2\theta - \sin^2\theta) = \dot{\sigma}t \cdot \cos 2\theta = \tau_{\parallel},
$$

$$
(31) \quad \vec{\tau} \cdot \widehat{l} = (\varrho gh \cdot \sin^2\theta + \dot{\sigma}t \cdot \cos\theta \cdot \sin\theta + \dot{\sigma}t \cdot \sin\theta \cdot \cos\theta + \varrho gh \cdot \cos^2\theta) =
$$

$$
= \varrho gh(\cos^2\theta + \sin^2\theta) + 2\dot{\sigma}t \cdot \sin\theta \cdot \cos\theta = \varrho gh + \dot{\sigma}t \cdot \sin 2\theta = \tau_{\perp}.
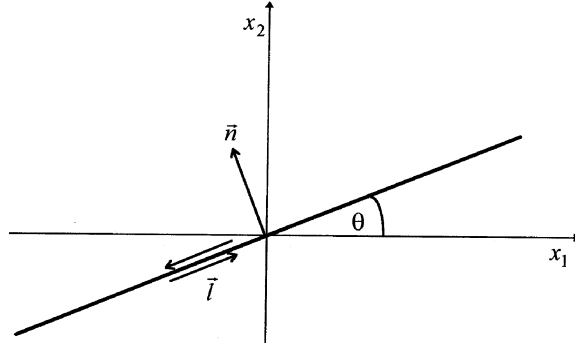$$

Fig. 2. – Fault direction in the (x_1, x_2)-plane. Faults are parallel to x_3; the shear is in the (x_1, x_2)-plane and parallel to x_1. In this co-ordinate system the faults are identified by the angle θ of their normal $\widehat{n}$ with the x_2-axis measured anticlockwise. The fault slip $\widehat{l}$ is also reported.

Comparing eqs. (29), (30) and (31) according to Caputo and Caputo [36], we see that

(32)
$$
\begin{cases}
F = \varrho g h \,, \\
f_c = f_0 \sin 2\theta \,, \\
f_c' = \cos 2\theta \,, \\
\beta = \dfrac{1}{1 - f_0 \tan 2\theta} \,,
\end{cases}
$$

where f_0 is the frictional coefficient between the faces of the fault.

Then, eqs. (22) become

(33)
$$
\begin{cases}
\dot{\sigma} t_n = \dfrac{F}{\sin 2\theta} \left[\dfrac{1}{(1 - f_0 \tan 2\theta)^n} - 1 \right], \\[2mm]
\dot{\sigma}(t_n - t_{n-1}) = \dfrac{F}{(1 - f_0 \tan 2\theta)^n \cos 2\theta} \,, \\[2mm]
p(t_n) = \dfrac{F}{(1 - f_0 \tan 2\theta)^n} = (F + f_0 \dot{\sigma} t_n \sin 2\theta) = \dot{\sigma}(t_n - t_{n-1}) \cos 2\theta
\end{cases}
$$

and eq. (24) can be written as

(34)
$$
n < - \frac{\log\left(1 + (T_1 \dot{\sigma} f_0 \sin 2\theta)/F\right)}{\log(1 - f_0 \tan 2\theta)} = \frac{\log(F/p(T_1))}{\log(1 - f_0 \tan 2\theta)} \,,
$$

where $p(T_1)$ is obtained from the third formula of eqs. (33) for $t_n = T_1$ (see also the following sect. 4).

Differentiating eq. (34) with respect to T_1, we obtain Omori's type law

(35)
$$
\frac{\mathrm{d}n}{\mathrm{d}T_1} = \frac{\mathrm{d}}{\mathrm{d}T_1} \left[\frac{\log\left((T_1 \dot{\sigma} f_0 \sin 2\theta)/F + 1\right)}{\log(\beta)} \right] =
$$

$$
= \frac{1}{\log(\beta)} \dot{\sigma} f_0 \sin 2\theta \frac{1}{T_1 \dot{\sigma} f_0 \sin 2\theta + F} \propto \frac{1}{T_1} \,,
$$

where we set, as in eq. (27), $(T_1 \dot{\sigma} f_0 \sin 2\theta)/F \gg 1$.

In order to have a first slip, the angle must satisfy one of the following conditions [36]:

(36)
$$
\begin{cases}
\left(0 < \theta < \dfrac{1}{2} a \tan\left(\dfrac{1}{f_0}\right)\right) + k\pi \,, \\[2mm]
\left(\dfrac{\pi}{2} - \dfrac{1}{2} a \tan\left(\dfrac{1}{f_0}\right)\right) < \theta < \dfrac{\pi}{2} + k\pi \,.
\end{cases}
$$

The value $\theta = (1/2) a \tan(1/f_0)$ is obtained by introducing eq. (29) in eq. (4), which gives $F + f_c \dot{\sigma} t_1 \sin 2\theta = f_c' \dot{\sigma} t_1 \cos 2\theta$, and assuming $t_1 = \infty$.
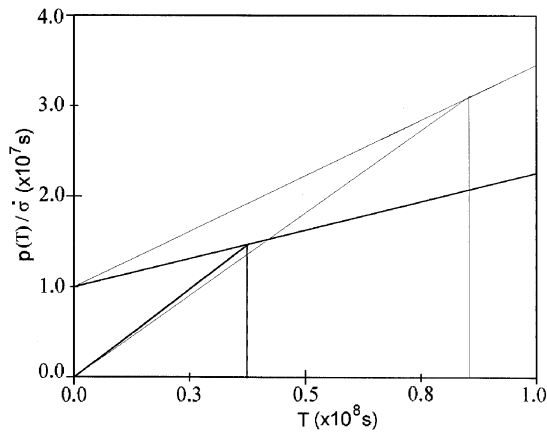
Fig. 3. – As in fig. 1 but taking into account eqs. (33) and (37) with $p(T_1) = 500\,F$, $F = 10^5$ Pa, $f_0 = 0.6$, and for two different values of θ ($\theta_1 = 6°$ and $\theta_2 = 12°$).

The maximum stress drop at the time T_1 is given by the value of $\sin 2\theta$ (for $\theta = \theta_1$), solution of the equation obtained substituting in the first formula of eqs. (33) $\dot\sigma t_n$ with $\dot\sigma T_1$ and assuming $n = 1$; in fact, it is seen from eqs. (33) that substituting this value of $\sin 2\theta$ in $p(t_n)$ the maximum stress drop in the time T_1 is obtained:

$$(37) \qquad \frac{\dot\sigma T_1}{F} = \frac{(P(T_1)/F - 1)}{f_0 \sin 2\theta_1} \,,$$

which implies that the time needed to reach the threshold of fracture, say $500\,F$, with $F = 10^5$ Pa, is inversely proportional to $\sin 2\theta$. This threshold represents the time intervals separating successive events and corresponding stress drops $p(t_n - t_{n-1})$ for several values of θ. For example, when we assume the same above-mentioned values, $p(T_1) = 500\,F$, $F = 10^5$ Pa, and $f_0 = 0.6$, the threshold is reached for $\theta = 6°$ when $\dot\sigma t/F = 4000$, while for $\theta = 12°$ it is reached when $\dot\sigma t/F = 2044$.

In fig. 3 we represent on the abscissa the numerical value of the very large increasing time separation between successive events when the stress drop limit is approached.

4. – The "catalogue" of earthquakes

We shall now obtain seismic events in the time interval from $t = 0$ through $t = T_1$ as a function of the seismic moment M_0 and of the strain energy W, assuming that the density distribution of the fault directions is constant, that the density distribution of the fault linear size l is given by eq. (1) and that all slips caused by the shear stress are as defined in the previous section. We shall also assume that the faults have homogeneous conditions of friction and are at the same depth h. However, this will not generate a real catalogue since we shall not consider the time of occurrence of each event.

On the fault with direction θ we have a number of slips n with stress drop p or smaller given by the value of n, satisfying inequality (34); we note that on each fault

the earthquake with minimum slip related to the direction of the fault, as well as the successive ones with increasing slip, occur only once.

As mentioned above, the number of events with stress drop p or smaller on the fault of direction θ is given by eq. (34) and the number of events of all the faults with the direction in the range $0 < \theta < (1/2)\, a\tan(1/f_0)$ is obtained integrating with respect to the following expression:

$$(38) \qquad n_p(p) = \int_0^{\theta_1} \frac{\log(F/p)}{\log(1 - f_0\tan 2\theta)}\, d\theta\,,$$

where θ_1 satisfies eq. (37). Then

$$(39) \qquad \theta_1 = \frac{1}{2}\, a\sin\left(\frac{p - F}{f_0\dot\sigma T_1}\right)$$

is obtained from eq. (37) with the above-mentioned conditions $n = 1$ and $T_1 = t_1$ corresponding to the maximum stress drop and to the occurrence of only one seismic event in the time interval $(0, T_1)$. Therefore, the upper limit of integration assures that there is at least one event with stress drop smaller than or equal to p. According to Caputo and Caputo [36], it may be seen from (39) that in the range $0 < \theta < (1/2)\, a\tan(1/f_0)$ at the same time, the faults with smaller θ have smaller stress drop; in the range $(\pi/2) - a\tan(1/f_0) < \theta < (\pi/2)$ the faults with larger θ have smaller stress drop, because in this case θ values are complementary to those considered in the previous case.

Differentiating $n_p(p)$ with respect to p in eq. (38) we obtain the density distribution of the stress drop:

$$(40) \qquad \overline{n}_p(p;\, 0,\, T_1) = \frac{dn_p(p)}{dp} = \frac{d}{dp}\left[-\int_0^{\theta_1} \frac{\log(1 + (f_0\dot\sigma T_1\sin 2\theta/F))}{\log(1 - f_0\tan 2\theta)}\, d\theta_1'\right]$$

and setting $X = (p - F)/F$ eq. (40) becomes

$$(41) \qquad \overline{n}_p(p;\, 0,\, T_1) = -\frac{\log(1 + X)}{\log\left(1 - \dfrac{XF/\dot\sigma T_1}{\sqrt{1 - (1/f_0^2)(XF/\dot\sigma T_1)^2}}\right)\left(2f_0\dot\sigma T_1\sqrt{1 - \dfrac{1}{f_0^2}\left(\dfrac{XF}{\dot\sigma T_1}\right)^2}\right)}\,.$$

In fig. 4 the function $\overline{n}_p(p;\, 0,\, T_1)$ is plotted for different values of $F/\dot\sigma T_1$. Then, it is verified by differentiating $n_p(p;\, 0,\, T_1)$ with respect to p, that $\overline{n}_p(p;\, 0,\, T_1)$ is decreasing for increasing $F/\dot\sigma T_1$ and that it has its maximum value $\overline{n}_p(p;\, 0,\, T_1) = 1/2f_0\dot\sigma T_1$, for $p = F$. For $4 \leqslant (p - F)/F \leqslant 10$ this function decreases as $1/p^s$ (fig. 5). The s factor assumes the values reported in table I. They refer to the three $F/\dot\sigma T_1$ values of fig. 4.

The empirical relationships [37, 38]

$$(42) \qquad \begin{cases} E = 10^{\beta + \gamma M} = \dfrac{\eta k}{2\mu}\, l^3 p^2 = \eta W\,, \\[2ex] M_0 = kl^3 p \end{cases}$$
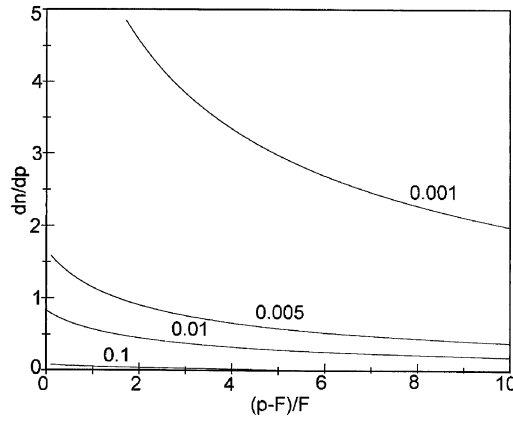
Fig. 4. – Plot of the density distribution function $\bar{n}_p(p; 0, T_1)$ of the stress drop p (see eq. (41)) in the time interval $(0, T_1)$ for three different values of $F/\dot{\sigma}T_1$ (equal to 0.001, 0.005, and 0.01).

relate the magnitude M, the radiated elastic energy E and the seismic moment M_0 to the linear fault dimension l, in a medium of rigidity μ for an event with stress drop p; η is the seismic efficiency, that is the factor accounting for the transformation of the
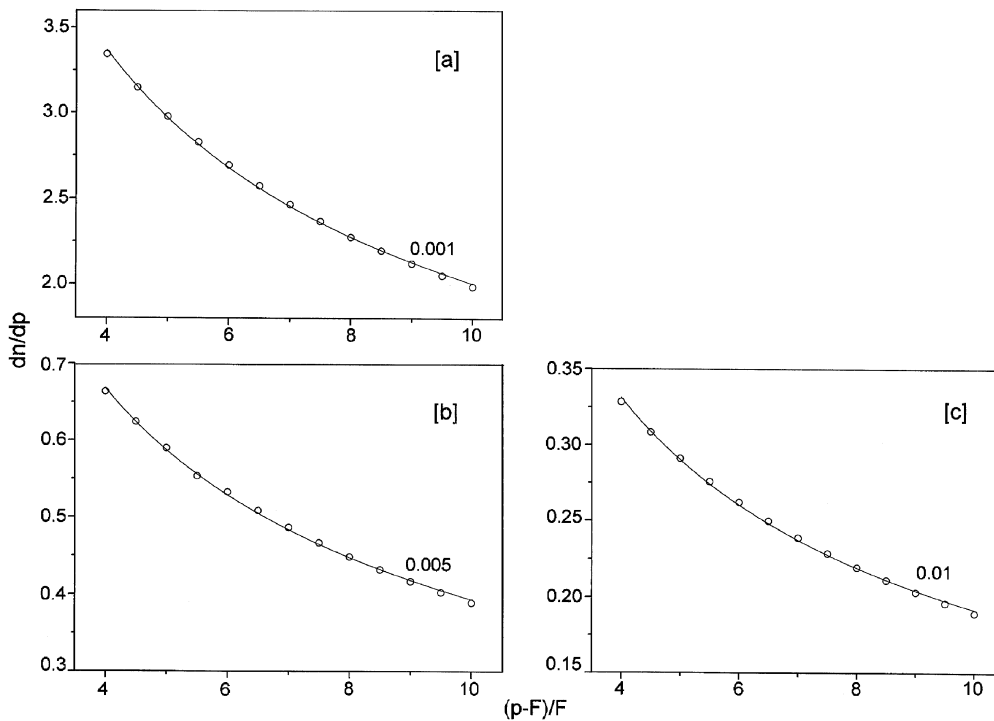

Fig. 5. – Best fitting of the density distribution function of the stress drop (eq. (41)) with the same three values of $F/\dot{\sigma}T_1$ reported in fig. 3 and for $4 \leq (p - F)/F \leq 10$. It is shown that this function decreases as $1/p^s$, where the s factor assumes the values reported in table I. a) Best fitting for $F/\dot{\sigma}T_1 = 0.001$; b) best fitting for $F/\dot{\sigma}T_1 = 0.005$; c) best fitting for $F/\dot{\sigma}T_1 = 0.01$.

TABLE I. – *Values of the parameters s and $F/\dot{o}T_1$ discussed in* eq. (41) *and concerning curves reported in figs.* 4 *and* 5.

s	$F/\dot{o}T_1$
0.56598	0.001
0.57755	0.005
0.5965	0.01

energy W stored in the elastic medium before the earthquake and released as seismic energy E into elastic waves; β and γ are parameters relating the energy E to the magnitude [38].

With these relations we may find the range of W for solving expression (37), as well as the range of seismic moment M_0.

As was shown by Caputo [30], it may be found that the logarithm of the density distribution of earthquakes is proportional to the logarithm of the energy W and to the logarithm of the seismic moment M_0, for finite intervals of W and M_0.

The cumulative distribution of the events (number of events) with $l_1 < l < l_2$ and $p_1 < p < p_2$ is then

$$(43) \qquad n(l, p; 0, T_1) = \int_{l_1}^{l_2} \int_{p_1}^{p_2} \overline{n}_p(p; 0, T_1)\, \overline{n}_l(l; 0, T_1)\, \mathrm{d}l\, \mathrm{d}p$$

with density distribution $\overline{n}_l = Dl^{-\nu}$.

The integration limits, l_1, p_1, l_2, p_2 are the minimum and the maximum fault size and stress drop, respectively; the values of these parameters can be approximated either from regional seismic catalogues, or on valuable data and field observations. In nature it seems that stress drops smaller than 10^4 Pa and larger than $5 \cdot 10^7$ Pa (which is about the breaking threshold of rocks) have not been observed yet. The fault length l may range from 10^{-3} m to 10^6 m, which can be realistically reduced to the range 1 m–10^4 m in order to account for much of the earthquakes [39].

The parameters l_1, l_2, p_1, p_2 define a rectangle A in the pl-plane, where every point represents an earthquake. The portion of this rectangle for solving the integral in eq. (43) is found by intersecting the rectangle A with the curve

$$(44) \qquad M_0 = kl_2^3 p \, ,$$

where the seismic moment is constant, in order to find the cumulative distribution with seismic moment less than M_0 (shaded portion in fig. 6). In the same way, by intersecting the rectangle A with the curve

$$(45) \qquad W = kl_2^3 p^2 \, ,$$

where the strain energy is constant, one can find the portion for solving the integral with strain energy less than W (shaded portion in fig. 7).

The two cases of interest for M_0 [30] are represented by the inequalities

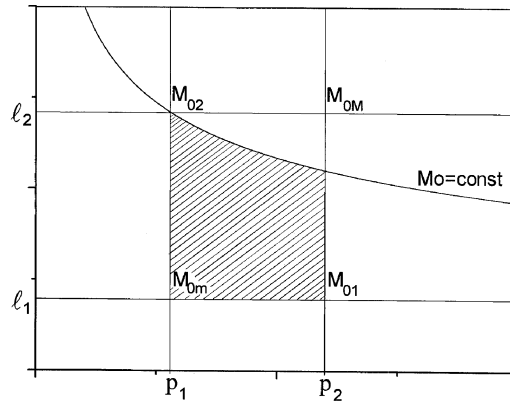$$(46) \qquad M_{01} = kl_1^3 p_2 \gtrless kl_2^3 p_1 = M_{02}$$

Fig. 6. – Plot of integral (43) where the integration limits l_1, p_1, l_2, p_2 are the minimum and maximum couple of values of fault size and stress drop, respectively. In the rectangle of the pl-plane every point represents an earthquake. The portion of this rectangle, for solving the integral (43), is found by intersecting the same rectangle with the curve $M_0 = kl_2^3 p$ (where the seismic moment M_0 is constant), in order to find the cumulative distribution with seismic moment less than M_0 (shaded area).

and the corresponding two ones, when using W, are

$$(47) \qquad\qquad W_1 = kl_1^3 p_2^2 \gtrless kl_2^3 p_1^2 = W_2.$$

By taking the derivative of eq. (43) with respect to M_0 it is verified (see appendix A) that the logarithm of the density distribution of M_0 is a linear function of $\log M_0$, in the interval $M_{01} < M_0 < M_{02}$, that is when $l_1^3 p_2 < l_2^3 p_1$. A similar function for the energy is found in the same way by taking the derivative with respect to W. It is also easily verified (appendix A) that, in general, outside the interval M_{01}, M_{02} (*i.e.*, outside W_1, W_2), this linearity does not exist [30].

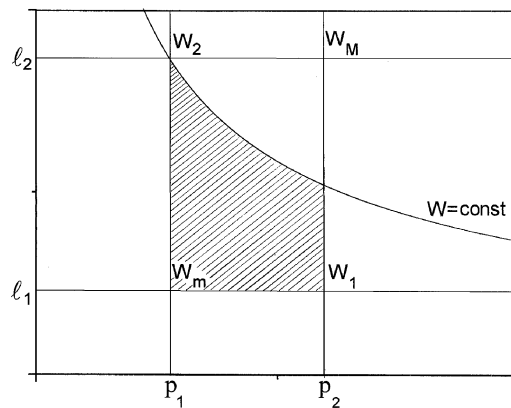
Fig. 7. – As in fig. 6 but intersecting the rectangle in the pl-plane with the curve $W = kl_2^3 p^2$ (where the strain energy W is constant).

5. – Discussion and conclusions

In the model of earthquake "catalogue" proposed here, we have found two different cases for the density distribution of seismic moment M_0 and other two for the density distribution of strain energy. It has been shown that, when $l_1^3 p_2 < l_2^3 p_1$,

(48)
$$
\begin{cases}
\log \bar{n}_0 \propto -\dfrac{\nu + 2}{3} \log M_0, \\[3mm]
\log \bar{n} \propto -\dfrac{\nu + 2}{3} \log W.
\end{cases}
$$

On the other hand, when $l_2^3 p_1 < l_1^3 p_2$, a similar linear relationship between $\log \bar{n}_0$ and $\log M_0$ and between $\log \bar{n}$ and $\log W$ does not exist. This is because on the basis of the above given values of the fault size and stress drop, we obtain that in nature $l_1^3 p_2 < l_2^3 p_1$ is the inequality to be satisfied most likely.

This implies that the seismic moment-frequency law found in this paper follows the Gutenberg-Richter empirical relationship, at least for the realistic values of the parameters l and p.

In this model, Omori's type law has also been verified.

By considering the events of two different time intervals $(0, T_1)$ and $(0, T_2)$ (with $T_2 > T_1$) both beginning at the time $t = 0$, by difference, one finds the events in the time interval (T_1, T_2). Its cumulative distribution is

(49)
$$
n(M_0; 0, T_2) - n(M_0; 0, T_1) = n(M_0; T_1 T_2)
$$

from which it follows, differentiating with respect to M_0, that also the log of the density distribution of the events in the time interval (T_1, T_2) is a linear function of $\log M_0$.

This implies that any catalogue of the events generated with this model, complete in a given time interval, has this property (self-similarity).

Taking into account the density distribution of the fault sizes, it may be observed that for $\nu = 1, 2, 3$ this distribution depends on the fault geometry, and in particular on length, on fault area, and on fault volume, respectively.

Experimental observations concerning ordinary earthquakes gave $\nu \cong 2.78$ [31]; ν-values greater than 3 correspond to b-values greater than those normally accepted on the basis of the Gutenberg-Richter relationship for ordinary seismic regions (where $b \approx 1$); then, ν-values greater than 3 do not have a simple physical or geometrical explanation. With respect to the case $\nu \leq 3$, they only ensure the activation of a major number of faults with smaller dimensions. On the basis of the relationships between ν, b, b_0, and γ, discussed in sects. **2** and **4**, it is evident that when $\nu > 3$, $b \cong 2$–2.5 and seismic swarms are obtained. The lower limit is constituted by the ideal case of an infinitive number of faults with infinitesimal dimension l which corresponds to the equipartition of energy and to a perfect seismic swarm manifestation.

When the stress drop is independent of the size of the faults, as one would have expected from eq. (44), the seismic moments scale as the volumes V.

This confirms that the linear relation appearing in the density distribution of $\log M_0$ is a property of geometric nature.

As concerns the evolution of the seismic region, the condition expressed by means of eq. (34), since the locking force is increasing with time and we have set a limit for the stress drop, seems to imply that the region, in spite of the increase of the stress field,

will eventually cease to have earthquakes except for the faults with direction $\theta = 0$ which have constant stress drop $p = F$, from the third equation of (33). However, even with the limit set for the stress drop, there is always a direction with an angle so small that the successive increases in stress drop are so small that stress drops smaller than the limit set are possible. However, this is due to the fact that we consider only earthquakes generated by existing faults.

The increase of the shear stress field applied to the region, when the shear stress will exceed the value of the assumed maximum stress drop p of the region and reach the threshold of fracture p_T, will eventually generate new faults and/or increase the length of the existing ones. An analysis of the maximum shear stress (mss) field generated by the slips along the existing faults and caused by a shear stress field indicates that at distance of about $10l$ from the end of the fault a large mss is generated with direction normal to the plane of the fault and to the plane of the shear [39].

The intensity of this mss may be tens of times the intensity of the field applied to the body, as was shown by Neuberg [40] and more recently by Caputo [41] and by Caputo and Console [42], who computed the mss of an elastic body containing an ellipsoidal cavity with symmetry of revolution around the x_1-axis, a semiaxis along x_1, l semiaxis along x_2, flattening $(l - a)/l = 0.99$, radius of curvature of the section normal to the equator at the equator $\varepsilon = l/a$, and subject to a shear stress field parallel to the equatorial plane of the cavity. Obviously, faults are not ellipsoidal cavities, but the tip border of faults will probably have a finite curvature which may be approximated with that of an ellipsoidal cavity at its equator.

On the basis of what mentioned above, new faults will therefore be generated, when the force needed to cause the slip reaches a value of several hundreds of the threshold value p_T. The new faults will have the same direction of the faults generating them, and therefore increase the population $Dl^{-\nu} \, dl$ of the existing ones. Although it seems that earthquakes with small stress drops are much more frequent than the earthquakes associated to large ones [31], the latter imply large values of the force needed to cause the slip, much larger mss near the tip of the fault and, as a consequence, the formation of new faults. It may be the set of newly formed faults which causes the set of shocks observed after strong earthquakes (aftershocks). Each of these faults will cause earthquakes with a distribution governed by formulae (22) and therefore, as we have already seen, in agreement with Omori's type law.

* * *

Appendix A

Let us demonstrate that the logarithm of $\overline{n}_0(M_0; 0, T_1)$ is a linear function of $\log M_0$ in the interval $M_{01} < M_0 < M_{02}$, that is when $l_1^3 p_2 < l_2^3 p_1$. A similar function for the energy W is found with the same conditions. On the contrary, when $M_{02} < M_0 < M_{01}$ and $W_2 < W < W_1$ the above-mentioned linearity does not exist.

Integrating first with respect to l, we obtain, in the interval $M_{01} < M_0 < M_{02}$ (that is, in the interval $W_1 < W < W_2$), the following expression for the cumulative distribution of M_0 (W):

$$(A.1) \quad n_0(M_0; 0, T_1) = D \int_{p_1}^{p_2} \overline{n}_p(p; 0, T_1) \, dp \int_{l_1}^{(M_0/kp)^{1/3}} l^{-\nu} \, dl =$$

$$= \frac{D}{\nu - 1} \left\{ \left(\frac{M_0}{k} \right)^{(1-\nu)/3} \int_{p_1}^{p_2} p^{(\nu-1)/3} \overline{n}_p(p; 0, T_1) \, dp - l_1^{1-\nu} [\overline{n}_p(p_2; 0, T_1) - \overline{n}_p(p_1; 0, T_1)] \right\}.$$

The density distribution $\overline{n}_0(M_0; 0, T_1)$ of earthquakes is

$$(A.2) \quad \overline{n}_0(M_0; 0, T_1) = \frac{\partial n_0(M_0; 0, T_1)}{\partial M_0} =$$

$$= \frac{D}{1-\nu} \left(\frac{1}{k} \right)^{(1-\nu)/3} M_0^{-(\nu+2)/3} \int_{p_1}^{p_2} p^{(\nu-1)/3} \overline{n}_p(M_0; 0, T_1) \, dp$$

and the logarithm of the density distribution, in the interval $M_{01} < M_0 < M_{02}$, is

$$(A.3) \quad \log [\overline{n}_0(M_0; 0, T_1)] = \log \left[\int_{p_1}^{p_2} (kp)^{(\nu-1)/3} \overline{n}_p(M_0; 0, T_1) \, dp \right] - \frac{\nu+2}{3} \log M_0,$$

which is a linear function of $\log M_0$.

In the same way

$$(A.4) \quad n(W; 0, T_1) = D \int_{p_1}^{p_2} \overline{n}_p(p; 0, T_1) \, dp \int_{l_1}^{(W/kp^2)^{1/3}} l^{-\nu} \, dl =$$

$$= \frac{D}{\nu - 1} \left\{ \left(\frac{W}{k} \right)^{(1-\nu)/3} \int_{p_1}^{p_2} p^{2(\nu-1)/3} \overline{n}_p(p; 0, T_1) \, dp - l_1^{1-\nu} [\overline{n}_p(p_2; 0, T_1) - \overline{n}_p(p_1; 0, T_1)] \right\}.$$

The density distribution $\overline{n}(W; 0, T_1)$ of earthquakes is

$$(A.5) \quad \overline{n}(W; 0, T_1) = \frac{\partial n(W; 0, T_1)}{\partial W} =$$

$$= \frac{D}{1-\nu} \left(\frac{1}{k} \right)^{(1-\nu)/3} W^{-(\nu+2)/3} \int_{p_1}^{p_2} p^{2(\nu-1)/3} \overline{n}_p(W; 0, T_1) \, dp$$

and the logarithm of the density distribution, in the interval $W_1 < W < W_2$, is

$$(A.6) \qquad \log[\overline{n}(W; 0, T_1)] = \log\left[\int_{p_1}^{p_2} (kp^2)^{(\nu-1)/3}\,\overline{n}_p(W; 0, T_1)\,\mathrm{d}p\right] - \frac{\nu+2}{3}\log W,$$

which is a linear function of $\log W$.

When the values l_1, l_2, p_1, p_2 are such that $l_1^3 p_2 > l_2^3 p_1$, which includes $M_{02} < M_0 < M_{01}$ and $W_2 < W < W_1$, by integrating first with respect to p we find

$$(A.7) \qquad n_0(M_0; 0, T_1) = D\int_{l_1}^{l_2} l^{-\nu}\,\mathrm{d}l \int_{p_1}^{(M_0/kl^3)} \overline{n}_p(p)\,\mathrm{d}p = D\int_{l_1}^{l_2} l^{-\nu}\left[n_p\left(\frac{M_0}{kl^3}\right) - n_p(p_1)\right]\mathrm{d}l =$$

$$= D\int_{l_1}^{l_2} n_p\left(\frac{M_0}{kl^3}\right) l^{-\nu}\,\mathrm{d}l - \frac{D}{1-\nu}\,n_p(p_1)[l_2^{1-\nu} - l_1^{1-\nu}]$$

and taking the derivative with respect to M_0 we obtain

$$(A.8) \qquad \overline{n}_0(M_0; 0, T_1) = \frac{\partial n_0(M_0; 0, T_1)}{\partial M_0} = D\int_{l_1}^{l_2} \frac{l^{-\nu}}{kl^3}\,\overline{n}_p\left(\frac{M_0}{kl^3}\right)\mathrm{d}l,$$

where, setting

$$Y = \frac{M_0}{kl^3} - F,$$

we have

$$(A.9) \qquad \overline{n}_0(M_0; 0, T_1) =$$

$$= D\left\{-\frac{\log(1+Y/F)}{\log\left(1+\left((YF/\dot{\sigma}T_1)\Big/\sqrt{1-\frac{1}{f_0^2}(YF)^2/(\dot{\sigma}T_1)^2}\right)\right)\left(2f_0\dot{\sigma}T_1\sqrt{1-\frac{1}{f_0^2}(YF)^2/(\dot{\sigma}T_1)^2}\right)}\right\}.$$

$$\cdot \int_{l_1}^{l_2} l^{-(\nu+3)}\,\mathrm{d}l.$$

Unlike what shown in eq. (A.3), the logarithm of the density distribution (eqs. (A.8), (A.9)) is not a linear function of $\log M_0$. In the Gutenberg-Richter relationship and seismic moment-frequency law, the parameter b is positive and $b_0 = 1 + b/\gamma$ assumes values greater than one. Moreover, the values found for the parameter s discussed in eq. (41) should be equal to those of b_0, being $s = b_0$ [31]. On the contrary, as may be seen in table I, s is of the order of 0.6.

In the same way, we find for the density distribution in the energy range W_2, W_1 (with $W_2 < W_1$), the following expressions:

$$(A.10) \quad n(W; 0, T_1) = D \int_{l_1}^{l_2} l^{-\nu} \, \mathrm{d}l \int_{p_1}^{(W_0/kl^3)^{1/2}} \overline{n}_p(p) \, \mathrm{d}p =$$

$$= D \int_{l_1}^{l_2} n_p\left(\left(\frac{W}{kl^3}\right)^{1/2}\right) l^{-\nu} \, \mathrm{d}l - \frac{D}{1-\nu} n_p(p_1)[l_2^{1-\nu} - l_1^{1-\nu}]$$

and taking the derivative with respect to W we obtain

$$(A.11) \quad \overline{n}(W; 0, T_1) = \frac{\partial n(W; 0, T_1)}{\partial W} = D \int_{l_1}^{l_2} \frac{l^{-\nu}}{kl^3} \overline{n}_p\left(\left(\frac{W}{kl^3}\right)^{1/2}\right) \, \mathrm{d}l \, ,$$

where, setting

$$Z = \left(\frac{W}{kl^3}\right)^{1/2} - F \, ,$$

we have

$$(A.12) \quad \overline{n}_0(W; 0, T_1) = D \int_{l_1}^{l_2} l^{-(\nu+3)}.$$

$$\cdot \left\{ - \frac{\log(1 + Z/F)}{\log\left(1 + \left((ZF/\dot{\sigma}T_1)\Big/ \sqrt{1 - \frac{1}{f_0^2}(ZF)^2/(\dot{\sigma}T_1)^2}\right)\right)\left(2f_0\dot{\sigma}T_1 \sqrt{1 - \frac{1}{f_0^2}(ZF)^2/(\dot{\sigma}T_1)^2}\right)} \right\} \mathrm{d}l \, ,$$

which is the same result obtained in eqs. (A.8) and (A.9) for M_0: the logarithm of the density distribution of the strain energy is not a linear function of $\log W$.

REFERENCES

[1] CAPUTO M., *Bull. Seism. Soc. Am.*, **67** (1977) 849.
[2] DAS S. and SCHOLZ C. H., *J. Geophys. Res.*, **86** (1981) 6039.
[3] KING C.-Y., *J. Geophys. Res.*, **96** (1991) 14377.
[4] KING G. C. P., STEIN R. S. and LIN J., *Bull. Seismol. Soc. Am.*, **84** (1994) 935.
[5] RICE J. R., *J. Geophys. Res.*, **98** (1993) 9885.
[6] ROBINSON R. and BENITES R., *J. Geophys. Res.*, **100** (1995) 18229.
[7] SENATORSKY P., *J. Geophys. Res.*, **100** (1995) 24111.
[8] WARD S. N., *J. Geophys. Res.*, **97** (1992) 6675.
[9] WARD S. N. and GOES S. D. B., *Geophys. Res. Lett.*, **20** (1993) 2131.
[10] GOES S. D. B., *J. Geophys. Res.*, **101** (1996) 5739.

[11] RUNDLE J. B., *J. Geophys. Res.*, **93** (1988) 6237.
[12] BARRIERE B. and TURCOTTE D. L., *Phys. Rev. E*, **49** (1994) 1151.
[13] CARLSON J. M., LANGER J. S., SHAW B. and TANG C., *Phys. Rev. A*, **44** (1991) 884.
[14] RUNDLE J. B. and KANAMORI H., *J. Geophys. Res.*, **92** (1987) 2606.
[15] REID H. F., in *The California Earthquake of April 18, 1906, Report of the State Investigation Commission* (Carnegie Institute of Washington, Washington, D.C.) 1910, pp. 1-192.
[16] MCCANN W. R., NISHENKO S. P., SYKES L. R. and KRAUSE J., *Pure Appl. Geophys.*, **117** (1979) 1082.
[17] NISHENKO S. P. and MCCANN W. R., in *Earthquake Prediction, An International Review, Maurice Ewing Series*, vol. **4**, edited by D. W. SIMPSON and P. G. RICHARDS (American Geophysisical Union, Washington, D.C.) 1981, pp. 20-28.
[18] SHIMAZAKI K. and NAKATA T., *Geophys. Res. Lett.*, **7** (1980) 279.
[19] LINDH A. G., *U.S. Geological Survey,* Open-File Report 83-63, 1984, pp. 1-14.
[20] SYKES L. R. and NISHENKO S. P., *J. Geophys. Res.*, **89** (19844) 5905.
[21] DIETERICH J. H., in *Intermediate-Term Earthquake Prediction*, edited by W. D. STUART and K. AKI, *Pure Appl. Geophys.*, **126** (1988) 589 (special issue).
[22] NEUMANN W. I. and KNOPOFF L., *Geophys. Res. Lett.*, **10** (1983) 305.
[23] ISHIMOTO M. and IIDA K., *Bull. Earthquake Res. Inst. Univ. Tokyo*, **17** (1939) 443.
[24] GUTENBERG B. and RICHTER C. F., *Seismicity of the Earth* (Princeton University Press, Princeton, N.J.) 1954, pp. 1-310.
[25] TRIEP E. G. and SYKES L. R., *J. Geophys. Res.*, **102** (1997) 9923.
[26] GUO Z. and OGATA Y., *J. Geophys. Res.*, **102** (1997) 2857.
[27] UTSU T., *Geophys. Magn.*, **30** (1961) 521.
[28] OKADA Y., *Bull. Seismol. Soc. Am.*, **82** (1992) 1018.
[29] CAPUTO M., *Ann. Geofis.*, **29** (1976) 277.
[30] CAPUTO M., in *Physics of Earth Interior*, edited by A. M. DZIEWONSKY and E. BOSCHI (North Holland, Amsterdam) 1980, pp. 669-688; *Tectonophys.*, **69** (1980) 9.
[31] CAPUTO M., *Geophys. J. R. Astron. Soc.*, **90** (1987) 551.
[32] DAVY P., *J. Geophys. Res.*, **98** (1993) 12141.
[33] CHRISTENSEN K and OLAMI Z., *J. Geophys. Res.*, **97** (1992) 8729.
[34] AKI K., *Pure Appl. Geophys.*, **145** (1995) 647.
[35] GABRIELOV A. M., LEVSHINA T. A. and ROTWAIN I. M., *Phys. Earth Planet. Inter.*, **61** (1990) 18.
[36] CAPUTO M. and CAPUTO R., *Boll. Geofis. Teor. Appl.*, **30** (1988) 395.
[37] KEILIS-BOROK V., *Ann. Geofis.*, **12** (1959) 205.
[38] BATH M., *Introduction to Seismology* (Birkhauser-Verlag, Basel) 1973.
[39] MORTENSEN C. E. and JOHNSTON M. J. S., *Pure Appl. Geophys.*, **113** (1975) 237.
[40] NEUBERG H., *Kerbspannunglehre* (Springer Verlag, Berlin) 1958.
[41] CAPUTO M., *Rend. Fis. Acc. Lincei*, **9** (1990) 357.
[42] CAPUTO M. and CONSOLE R., *Stress field, deformations and displacements around a cavity in an elastic medium*, submitted, 1999.